Influence of Pt loading on Al_2O_3 for the low temperature combustion of methanol with and without a trace amount of ammonia

Andreas Hinz [a], Per-Olof Larsson [b], and Arne Andersson [a]

[a] *Department of Chemical Engineering II, Lund University, Chemical Center, PO Box 124, SE-221 00 Lund, Sweden*
[b] *Perstorp Catalysts, Perstorp AB, SE-284 80 Perstorp, Sweden*

Received 10 July 2001; accepted 3 October 2001

Pt/Al_2O_3 catalysts with platinum contents of 0.1, 1.0 and 3.0 wt% were used for the low temperature combustion of methanol in the absence and the respective presence of a trace amount of ammonia. It is observed that ammonia inhibits the combustion of methanol, which is due to competition between methanol and ammonia for the same sites. For a fixed space velocity and without ammonia in the gas, the performances of the catalysts increase up to a Pt loading of 1.0 wt%. In the presence of ammonia, however, no upper limit of performance is observed with increased Pt content. The results are discussed in terms of both Pt–support interface and the Pt surface being active.

KEY WORDS: methanol; combustion; Pt/Al_2O_3; poisoning; ammonia; metal–support interface

1. Introduction

Pt/Al_2O_3 catalysts are well known [1–4] to be active for the combustion of methanol and formaldehyde at low temperature. An advantage of catalytic incineration, compared with thermal incineration and flame combustion, is to save resources by burning the organic pollutants at the off-gas temperature in the diluted gas stream [5]. However, the reaction temperature being required for catalytic combustion depends on the catalyst poisons being present in the waste gas and the content of platinum on the catalyst. For example, the off-gas from melamine laminate impregnation plants contains methanol, formaldehyde and amine compounds. As ammonia and related compounds are known to be poisons for Pt/Al_2O_3 [6,7], the low temperature combustion of the waste gas is not straightforward.

For supported metal catalysts it has been demonstrated that the metal particle size is a factor affecting the catalytic performance. In that case the reaction is structure sensitive and the rate-limiting step is believed to involve an ensemble of atoms [8]. Examples of such reactions on Pt/Al_2O_3 are the oxidation of methane [9], propane [10], benzene [11], and ethyl acetate [11], while the oxidation of butanol was found to be structure-insensitive [11]. For a structure-insensitive reaction it is believed that only one metal atom is involved in the rate-limiting step [8]. In other instances there is evidence for the reaction taking place at the interface between the metal and the support [12], *e.g.*, the ring opening of methyl cyclopentane on supported Pt. Another phenomenon of relevance for catalysis on supported metal catalysts is the spillover of species from one phase to the other. For instance, in the oxidation of VOCs, including methanol, over Ag/Al_2O_3 it was inferred that there is diffusion of adsorbed intermediates from the support surface to the active Ag sites [5].

The objective of this paper is to examine the combustion of methanol over Pt/Al_2O_3 catalysts with different loads of platinum, an issue that is relevant for industrial applications. Catalytic experiments were performed in the presence and, respectively, absence of ammonia, reflecting the poisoning effect that is caused by amine compounds.

2. Experimental

2.1. Preparation of catalysts

The support material was obtained by crushing and screening Al_2O_3 spheres (Alcoa) to the desired 250–425 μm particle size fraction. Thereafter, 25 ml of the support material was treated with 100 ml of distilled water to wash the particles and fill the pores. The solid material was then filtered off and added to 100 ml of an appropriate platinum(II) nitrate solution, which was prepared by diluting a 15.23 wt% $Pt(NO_3)_2$ solution from Heraeus with water. Samples with a loading of 1, 10, or 30 mg-Pt/g of support were prepared. To promote the interaction between the anionic Pt-complex and the positively charged support surface [13], the pH value of the slurry was initially adjusted to 1.9 by adding either 1 M HNO_3 or 2.5% NH_3 in water solution. For 1 h the slurry was shaken by hand every fifth minute to ensure that the adsorption of Pt onto the support was complete. After the impregnation, the slurry was filtered and the solid residue was dried in an oven for 1 h at 100 °C. Then, the material was calcined under flowing air for 1.5 h at 500 °C and finally reduced in flowing hydrogen for 1 h at 450 °C.

2.2. Catalytic tests

The catalytic tests were performed under adiabatic steady state conditions in a cylindrical reactor made of stainless

steel. To obtain better adiabatic conditions, the reactor was surrounded with an insulation section, which was heated to the temperature of the inlet gas. All other pipes of the system were heated to avoid condensation. In the experiments a 20 l(STP)/min flow of industrial air free of CO_2 and with either 300 ppm methanol and 2000 ppm water, or 300 ppm methanol, 3 ppm ammonia, and 1997 ppm water was passed over 15 ml catalyst, giving a gas hourly space velocity (GHSV) of 80 000 h^{-1}. The airflow was controlled by a mass flow controller (Brooks) and liquid components were fed by a liquid pump (Alitea) that pumped either a mixture of methanol and water or methanol, water and ammonia solution into an evaporator where mixing with air occurred. The resulting gas mixture was then passed through an electric preheater before entering the reactor. The temperature was measured with two thermocouples, which were located in front of and after the catalytic bed, respectively.

Continuous gas analyses were performed at the outlet and the inlet of the reactor. CO_2 was analysed by passing a gas flow of 0.5 l/min through, first, a condenser (Insat AG, JCP-FE) and, then, through an IR instrument (Fuji electronic, ZRF IR-analyser). Analysis of the inlet concentration of methanol was performed, by passing a gas flow of 1.5 l/min directly through an FID detector (Bernath Atomic, model 3006).

2.3. Characterisation of catalysts

A TAP-2 reactor system [14] equipped with a UTI 100C mass spectrometer was used to perform temperature-programmed desorption (TPD) experiments. Before running a TPD experiment, the catalyst (200–235 mg) was first pre-treated with oxygen. For this purpose, a 40 ml/min flow of oxygen was led over the catalyst for 10 min at 450 °C. Then, the temperature was decreased to 50 °C in flowing argon (32 ml/min). After the pre-treatment was finished, the catalyst was submitted for 45 min to either a flow (52 ml/min) of argon with 0.4 vol% methanol, or a flow (56 ml/min) of argon with 0.4 vol% methanol and 7.1 vol% ammonia. Finally, the reactor was evacuated and the temperature was increased linearly by 10 °C/min from 50 up to 400 °C. During the TPD experiment, the scanning range of the mass spectrometer was set to the m/e ratio (amu) ranges 0–8, 11–21, 24–34, and 37–50, including all masses of interest.

X-ray photoelectron spectroscopy (XPS) spectra were recorded with a Kratos XSAM 800 spectrometer using a Mg Kα anode (1253.6 eV) operating at an acceleration voltage of 13 kV and a current of 20 mA. Fresh catalyst samples were used for the analyses, which comprised the recording of a wide scan of the 0–1100 eV region of binding energy and single scans of the O 1s, Pt $4d_{5/2}$, Al 2s, and C 1s regions. Charging effects were corrected for by adjusting the C 1s peak to a position of 285.0 eV.

A Micromeritics ASAP 2400 instrument was used to measure the specific surface area (BET), the pore volume and the pore size distribution in the range 17–3000 Å. The measurements were performed on freshly prepared catalysts, which had been degassed at 350 °C for 16 h, by recording the adsorption and desorption isotherms of N_2 at the temperature of liquid nitrogen. The pore volumes and pore size distribution were calculated with the method of Barrett *et al.* [15].

To determine the dispersion and surface area of the platinum in the catalyst, the chemisorption of CO was measured at 35 °C using a Micromeritics ASAP 2010 instrument. From the measured values, the dispersion and surface area of the platinum were calculated using a stoichiometry factor of one adsorbed CO molecule per Pt surface atom [16] and an area of 0.08 nm^2 per Pt atom [17].

X-ray diffraction (XRD) analyses were carried out with Ni-filtered Cu Kα radiation on a Seifert XRD 3000 TT diffractometer. The measurements of the support and the prepared catalysts showed broad diffraction peaks from γ-Al_2O_3 [18] only. No diffraction lines from Pt metal were visible due to the low loading of Pt.

3. Results

3.1. Specific surface area, pore size, pore volume, and dispersion of platinum

The results obtained by the N_2 adsorption and CO chemisorption measurements are shown in table 1. It appears that the values for the BET surface area, the pore size distribution, the pore volume and the dispersion of Pt are almost independent of the platinum content on the support. The surface area that is covered with Pt increases approximately linearly with the Pt content of the catalyst.

Table 1
Results of the N_2 adsorption and CO chemisorption measurements

Catalyst	BET surface area[a] (m^2/g)	Pore size distribution[b] (Å)	Pore volume[c] (cm^3/g)	Pt dispersion (%)	Pt surface area (m^2/g)
Al_2O_3	157	45–950 (85, 160)	0.44	–	–
0.1 wt% Pt/Al_2O_3	158 (158)	45–950 (85, 160)	0.44	26.41	0.0652
1.0 wt% Pt/Al_2O_3	161 (163)	45–1000 (85, 160)	0.45	27.68	0.6838
3.0 wt% Pt/Al_2O_3	149 (154)	45–950 (85, 160)	0.42	30.58	2.2657

[a] The specific surface area in m^2/g of catalyst, and in parentheses in m^2/g of support.
[b] The pore diameter at the adsorption distribution maxima are given in parentheses.
[c] The adsorption pore volume for the 17–3000 Å range of pore diameters.

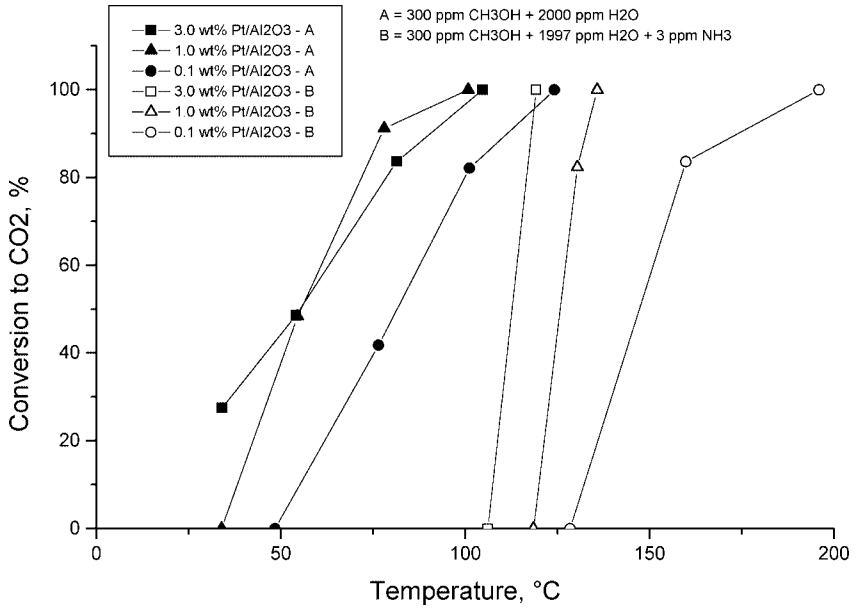

Figure 1. Conversion of methanol to CO_2 in the presence and the respective absence of NH_3 over 0.1, 1.0, and 3.0 wt% Pt on Al_2O_3. The feed compositions are displayed in the figure.

3.2. Total oxidation of methanol to CO_2

Methanol combustion was performed on the Pt/Al_2O_3 catalysts in both the absence and the presence of trace amounts of ammonia. Figure 1 shows the data obtained for the conversion of methanol to CO_2 as a function of the temperature. In the absence of NH_3, the figure shows that for high conversions to CO_2 the performance of the Pt/Al_2O_3 catalysts increases in the order 0.1 wt% Pt $<$ 1.0 wt% Pt $\approx$ 3.0 wt% Pt. At low temperatures the 3.0 wt% Pt/Al_2O_3 catalyst exhibits the best performance. When trace amounts of NH_3 are present in the feed, the conversion curves are shifted towards higher temperature. Moreover, the performance of Pt/Al_2O_3 decreases with the Pt content in the order 3.0 wt% Pt $>$ 1.0 wt% Pt $>$ 0.1 wt% Pt.

3.3. X-ray photoelectron spectroscopy

The Pt $4d_{5/2}$ binding energy seemed to be independent of the platinum content on the Al_2O_3 support and the measured value was 315.2, 315.5, and 315.4 eV for 0.1, 1.0, and 3.0 wt% Pt/Al_2O_3, respectively. For the same samples, according to XPS the surface content of Pt increased with the nominal loading and was 2.20, 3.34, and 13.25 at%, respectively.

3.4. Methanol TPD experiments

In figure 2 the TPD responses after adsorption of methanol are shown. The largest amounts of formaldehyde and dimethyl ether (DME) are produced and desorb from the 0.1 wt% Pt/Al_2O_3 catalyst and both amounts decrease with an increased loading of platinum on the support. The opposite behaviour with the Pt content is largely visible for the responses of hydrogen, CO and CO_2. Also it is noteworthy that the amount of desorbed methanol is almost unaffected by the Pt content on the Al_2O_3 surface.

In figure 3 are the TPD responses shown after co-adsorption of methanol and ammonia. Compared to the responses in figure 2, those in figure 3 are less intense and the response peaks from dimethyl ether and formaldehyde are shifted towards higher temperature. Moreover, the co-adsorption of ammonia alters the shape of the response curves from the signals at 2 (H_2), 28 (CO/N_2) and 44 (CO_2/N_2O) amu.

4. Discussion

The TPD results in figure 2, which were recorded after methanol treatment of the oxidised catalysts in the absence of ammonia, show that methanol is adsorbed both reversibly and irreversibly on the Pt/Al_2O_3 surface. A part of the adsorbed methanol is decomposed to CO and H_2 as evidenced by the similarity of the profiles of the two products. Another part of the methanol forms dimethyl ether and formaldehyde, products which like CO are further oxidised to form CO_2. The profiles of dimethyl ether and formaldehyde appear at the same temperature and are almost identical in shape, indicating that these products are formed from the same intermediate species. This species is possibly a methoxy species, the formation of which is rate determining.

A comparison of the TPD profiles in figure 3 with those in figure 2 demonstrates that the co-adsorption of ammonia with methanol leads to less methanol being desorbed. Moreover, the formations of dimethyl ether and formaldehyde are reduced, especially in case of 0.1 wt% Pt/Al_2O_3. The m/e signals 2 (H_2), 28 (CO, N_2), and 44 (CO_2, N_2O) amu in figure 3 are less informative since these include the

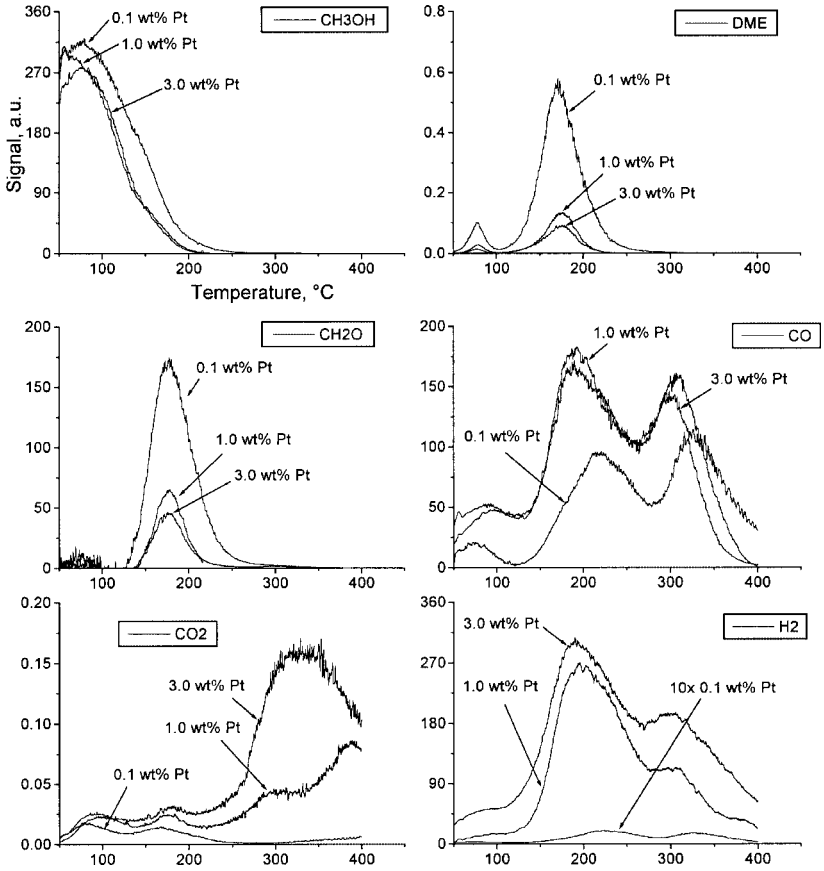

Figure 2. TPD profiles of methanol and products formed during TPD after adsorption of methanol at 50 °C onto the pre-oxidised catalysts. The profiles have been normalised with respect to differences in gain and surface area of the catalyst.

contribution from the conversion of both methanol and ammonia. However, comparing the CO signal in figure 2 with the 28 amu signal (CO/N_2) in figure 3 it is seen that the co-adsorption of ammonia on the Pt/Al_2O_3 surface inhibits the formation of CO from methanol. From the TPD results it can be concluded that the retardation by ammonia of the methanol combustion, which is observed in figure 1, is in part due to ammonia competing with methanol for the same adsorption sites [19].

The product spectrum as it appears in figures 2 and 3 is consistent with previous reports. It has, for example, been reported that the decomposition of methanol produces H_2, CO, dimethyl ether, and CO_2 on both Al_2O_3 [19,20] and Pt/Al_2O_3 [19,21]. Over unsupported Pt, the decomposition of methanol primarily gives H_2 and CO [22,23]. If there is oxygen on the surface then CO_2 [23] and formaldehyde [24] can form as well. Formation of formaldehyde takes place on the Pt(110) face [24] but not on the Pt(100) [23] and Pt(111) [22,25] surfaces.

Concerning the TPD profiles in figures 2 and 3 it should be noticed that the amount of adsorbed methanol is almost unaffected by the Pt content on Al_2O_3 and, moreover, the amount did not differ considerably from that being observed for the bare alumina. This finding is consistent with our previous results for 0.1 wt% Pt/Al_2O_3 showing that most of the methanol is adsorbed on the support surface [19]. Considering the profiles for dimethyl ether and formaldehyde, these rather indicate that both products are primarily formed on the Al_2O_3 surface since the integrated signals decrease with increase of the Pt content. Moreover, as discussed above, the correspondence between the profiles indicates that these products are formed from a common intermediate. However, from the observation that the peak temperature for dimethyl ether and formaldehyde desorption from Pt/Al_2O_3 is 175 °C (figure 2) to be compared with approximately 250–300 °C for Al_2O_3 [19,20], it can be suggested that the precursor species is formed on the support surface and migrates to react at the Pt–alumina interface or the platinum surface. Similar results, *i.e.*, spillover of adsorbed species from the support to the active material where the species react, have been observed to take place in methanol combustion over other catalyst systems, *e.g.*, Ag/Al_2O_3 [5], Pd/Al_2O_3 [20], and CuO/Al_2O_3 [26]. As opposed to the formations of dimethyl ether and formaldehyde, figure 2 shows that the formations of hydrogen and carbon oxides ($CO + CO_2$) increase with the Pt content of the catalyst. The opposite trends with the Pt content are in support of the Pt in Pt/Al_2O_3 being active for the decomposition of methanol to H_2 and CO and the consecutive oxidation of dimethyl ether, formaldehyde and CO to give CO_2. Further evidence for Pt being involved in the decomposition of methanol is that the CO profile in figure 2 has a peak around 200 °C, which is the same temperature

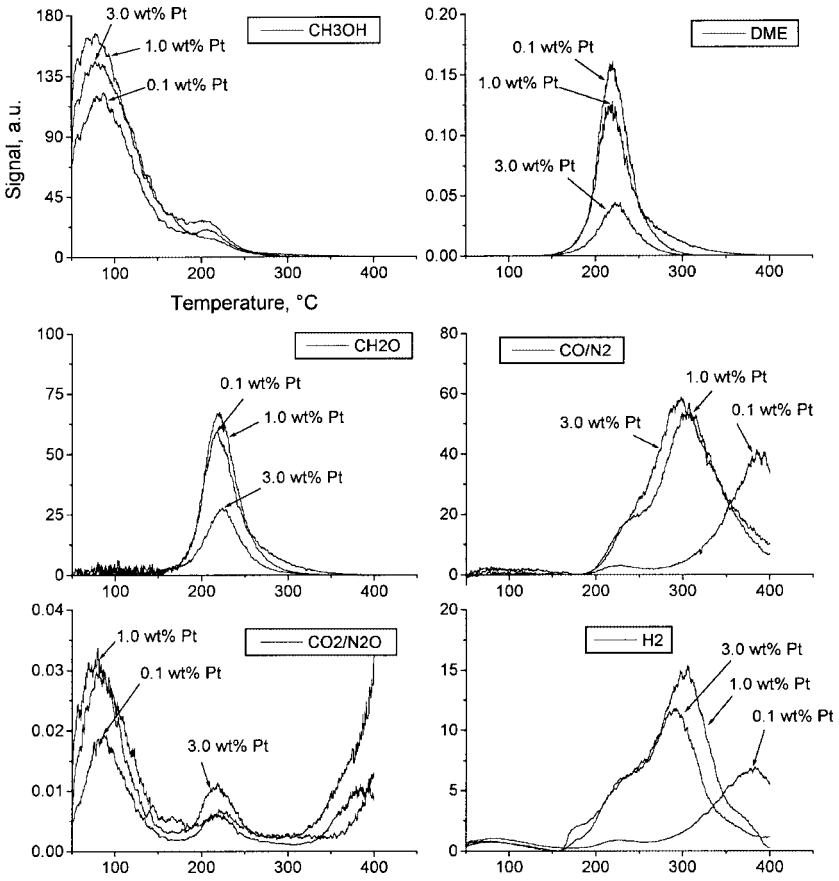

Figure 3. TPD profiles of methanol and products formed during TPD after co-adsorption of methanol and ammonia at 50 °C on the pre-oxidised catalysts. The profiles have been normalised with respect to differences in gain and surface area of the catalyst.

as being reported for the desorption of CO when methanol decomposes on Pt metal [22].

The data in table 1 show almost unchanged Pt dispersion with increase of the Pt content on the alumina support. This finding is consistent with previous reports [9,27] showing a transition point between dispersed and particulate Pt on alumina at approximately 2 μmol-Pt/m^2 (BET). For the alumina being used in the present investigation, 3 wt% of Pt corresponds to 1 μmol-Pt/m^2 (BET). Considering that the dispersion of Pt is the same on the Pt/Al_2O_3 catalysts, it can be assumed that the Pt crystallites of the samples are of the same size. Then, as the catalytic data in figure 1 for the Pt/Al_2O_3 catalysts were measured at a fixed space velocity, the performances of the catalysts should be expected to increase with increase of the Pt content on the support. This expectation is obvious since the used space velocity of 80 000 h^{-1} corresponds to a total Pt surface area in the reactor of 0.61, 6.84, and 22.05 m^2 for the catalysts with a Pt content of 0.1, 1.0, and 3.0 wt%, respectively. For the complete combustion of methanol to CO_2 in the presence of ammonia, the catalytic data in figure 1 reflect well the differences in Pt content of the Pt/Al_2O_3 catalysts and the catalytic performance is improved with an increase of the Pt content. However, the catalytic data for methanol combustion in the absence of ammonia cannot be explained fully by the different surface areas of Pt. In this case, figure 1 shows that the efficiency of the catalyst tends to a limiting value when the Pt content is increased, *i.e.*, the conversion curve almost does not shift towards lower temperatures as the Pt content is increased above 1 wt%. Thus, the order of performance among the Pt/Al_2O_3 catalysts becomes $0.1 < 1.0 \approx 3.0$ wt% Pt. The existence of an upper limit for the catalytic performance with increase of the Pt content cannot be explained by any difference in Pt dispersion, surface area, pore-size distribution, pore volume (tables 1) or Pt $4d_{5/2}$ binding energy. However, for supported metal catalysts it is known from the literature that many reactions are believed to proceed at the metal–support interface [12]. In the following it will be demonstrated that the catalytic data in figure 1 can be explained by the sites at the Pt–Al_2O_3 borderline being active for methanol combustion in the absence of ammonia.

Investigation of the present catalysts with TEM microscopy showed that the support crystallites are in the form of disordered needles [19]. However, no Pt crystallites could be resolved in any of the three Pt/Al_2O_3 samples, which can be due to the difference in contrast being small between Pt and Al_2O_3 since the support crystallites are not well crystalline and the Pt particles are small. On the other hand, in previous investigations with scanning tunneling [28] and transmission electron microscopy [29] of Pt deposited onto a thin and ordered film of Al_2O_3 grown on a NiAl(110) sur-

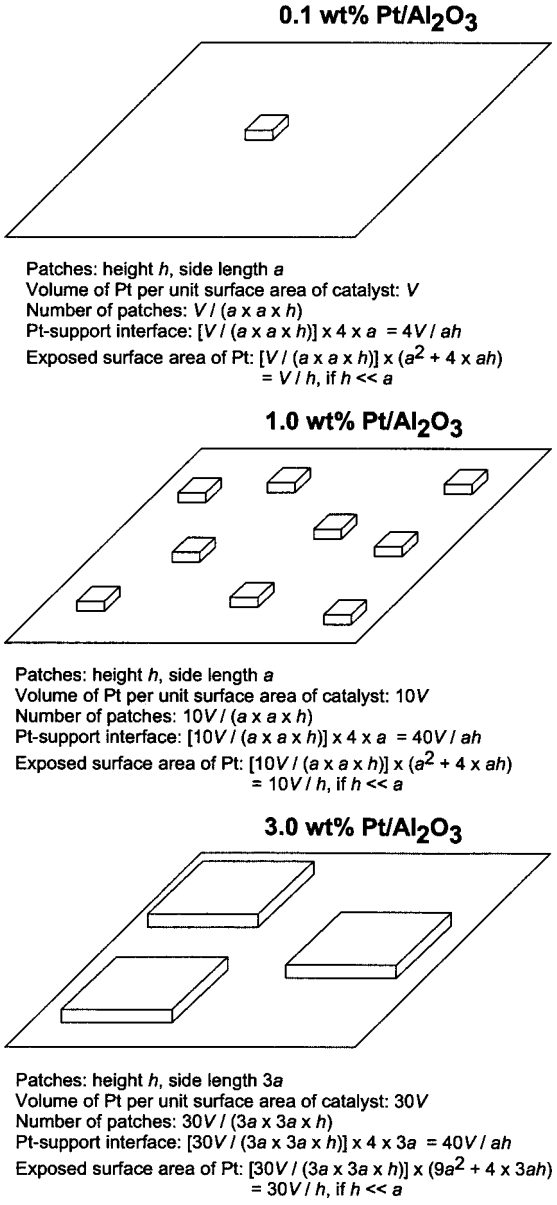

Figure 4. A model of the Pt/Al_2O_3 surface with thin two-dimensional patches of platinum interacting with the support. With increase of the Pt loading from 0.1 to 1.0 wt% the number of small patches is increased. Above 1.0 wt% of Pt the small patches start to coalesce into larger patches with unchanged thickness. As the patches are thin, the surface area of the Pt being exposed increases almost proportionally with the Pt content. However, the Pt–Al_2O_3 interface tends to a limiting value.

face it has been shown that platinum up to a coverage of one monolayer on Al_2O_3 forms flat, highly dispersed two-dimensional islands with a height of 1.5–4 Å and comprising 20–50 Pt atoms. Compared with bulk Pt, the interatomic distances in the islands are smaller, suggesting a partly reduced electron density on the Pt aggregates [29]. This inference is consistent with the Pt $4d_{5/2}$ binding energy values for the present samples. The values 315.2–315.5 eV indicate that the Pt strongly interacts with the support considering that the corresponding binding energy is 314.5, 317.1, and 318.4 eV for Pt^0, Na_2PtCl_4, and PtO_2 [30], respectively, using C 1s at 285.0 eV as reference. Interaction between Pt and Al_2O_3 through Pt–O–support bonding has been proposed in previous investigations considering EXAFS results [31] and the X-ray induced O KVV Auger transition [32]. On the basis of these findings, the model of the catalyst surface in figure 4 is proposed for 0.1, 1.0, and 3.0 wt% of Pt on Al_2O_3. Highly dispersed patches of Pt are formed, which are linked to the support through bridging oxygen. The patches are thin due to Pt–support interaction and, therefore, the side faces are small compared to the large basal plane. When the Pt loading is increased from 0.1 to 1.0 wt% Pt, the size of the patches remains unchanged and the number of patches increases by a factor ten and so do the exposed Pt surface area and the number of Pt–support interface sites. With further increase of the Pt content from 1.0 to 3.0 wt%, the smaller patches coalesce to larger ones. If it is assumed that the basal plane is enlarged a factor nine, then the number of Pt–support interface sites will be unchanged but the Pt surface area will increase by a factor three approximately (see figure 4). Assuming that the Pt–Al_2O_3 borderline sites are much more active than the Pt surface sites for the combustion of methanol in the absence of ammonia, then the model explains the variation of the catalytic performance with the Pt content on Al_2O_3 as it appears from the plots in figure 1. Moreover, the catalytic data in figure 1 for methanol combustion in the presence of ammonia agree with the Pt surface in this case being active since it increases proportionally with the Pt content on Al_2O_3.

The inference that, depending on whether ammonia is present in the gas, different types of active sites operate for methanol combustion can be explained by the ammonia being adsorbed and reacting preferentially on the Pt–alumina borderline sites. As a consequence, methanol conversion at these the most active sites is prevented, which leads to the methanol being combusted at the less active Pt surface sites. This interpretation agrees with previous results for Pt/Al_2O_3 showing that ammonia is preferably adsorbed at the Pt–alumina boundary [33]. Moreover, the results are consistent with the present TPD measurements, see figures 2 and 3, showing a competition between methanol and ammonia for adsorption sites. The strong inhibition of the methanol combustion by a trace amount of ammonia, which is seen in figure 1, is in support of the most active sites being poisoned by ammonia. The indication obtained from the TPD results in figure 2, namely that there are different reaction pathways involving interfacial and Pt surface sites, respectively, are consistent with the involvement of two types of sites with different reactivity. It is reasonable that the activation energies for methanol combustion differ on the two types of sites, which is suggested by the TPD profiles for CO_2 in figure 2 showing an increase of the CO_2 signal with an increase of the Pt content on the support. In this case there is no tendency towards a limiting value, which can be due to the fact that there is no oxygen in the gas phase and, consequently, CO_2 is formed at a higher temperature than is the case in the stationary experiments (figure 1). At the higher temperature it seems that the Pt surface sites are more active (*cf.* the model in figure 4), indicating that the activation energy for

methanol combustion is higher on the Pt surface sites than on the Pt–support borderline sites.

Acknowledgment

Perstorp AB and the Swedish Research Council for Engineering Sciences (TFR) are acknowledged for financial support. We are grateful to Mrs. Birgitta Svensson for performing the nitrogen adsorption and CO chemisorption measurements.

References

[1] R.W. McCabe and P.J. Mitchell, Appl. Catal. 44 (1988) 73.
[2] D. Sodhi, M.A. Abraham and J.C. Summers, J. Air Waste Manage. Assoc. 40 (1990) 352.
[3] K. Munkata, M. Sasaki and T. Ito, Appl. Catal. B 4 (1994) 315.
[4] R.K. Sharma, B. Zhou, S. Tong and K.T. Chuang, Ind. Eng. Chem. Res. 34 (1995) 4310.
[5] E.M. Cordi and J.L. Falconer, Appl. Catal. A 151 (1997) 179.
[6] J.J. Ostermaier, J.R. Katzer and W.H. Manogue, J. Catal. 41 (1976) 277.
[7] J.C. Luy and J.M. Parera, Appl. Catal. 13 (1984) 39.
[8] M. Boudart, in: *Proc. 6th Int. Congr. on Catalysis*, Vol. 1, eds. G.C. Bond, P.B. Wells and F.C. Tompkins (The Chemical Society, London, 1977) p. 1.
[9] K. Otto, Langmuir 5 (1989) 1364.
[10] K. Otto, J.M. Andino and C.L. Parks, J. Catal. 131 (1991) 243.
[11] P. Papaefthimiou, T. Ionnides and X.E. Verykios, Appl. Catal. B 13 (1997) 175.
[12] K. Hayek, R. Kramer and Z. Paál, Appl. Catal. A 162 (1997) 1.
[13] T. Mang, B. Breitscheidel, P. Polanek and H. Knözinger, Appl. Catal. A 106 (1993) 239.
[14] J.T. Gleaves, G.S. Yablonskii, P. Phanawadee and Y. Schuurman, Appl. Catal. A 160 (1997) 55.
[15] E.P. Barrett, L.G. Joyner and P.H. Halenda, J. Am. Chem. Soc. 73 (1951) 373.
[16] R.W. McCabe and D.F. McCready, J. Phys. Chem. 90 (1986) 1428.
[17] Micromeritics, Operator's manual to the ASAP 2010 chemi system, Norcross, GA, 1994.
[18] JCPDS International Centre for Diffraction Data, Powder diffraction file, Swarthmore, PA, 1991.
[19] A. Hinz, P.-O. Larsson, B. Skårman and A. Andersson, Appl. Catal. B, in press.
[20] E.M. Cordi and J.L. Falconer, J. Catal. 162 (1996) 104.
[21] S. Imamura, T. Higashihara, Y. Saito, H. Aritani, H. Kanai, Y. Matsumura and N. Tsuda, Catal. Today 50 (1999) 369.
[22] B.A. Sexton, Surf. Sci. 102 (1981) 271.
[23] N. Kizhakevariam and E.M. Stuve, Surf. Sci. 286 (1993) 246.
[24] J. Wang, M.A. DeAngelis, D. Zaikos, M. Setiadi and R.I. Masel, Surf. Sci. 318 (1994) 307.
[25] M. Endo, T. Matsumoto, J. Kubota, K. Domen and C. Hirose, Surf. Sci. 441 (1999) L931.
[26] E.M. Cordi, P.J. O'Neill and J.L. Falconer, Appl. Catal. B 14 (1997) 23.
[27] H.C. Yao, M. Sieg and H.K. Plummer, J. Catal. 59 (1979) 365.
[28] Th. Bertrams, F. Winkelmann, Th. Uttich, H.-J. Freund and H. Neddermeyer, Surf. Sci. 331 (1995) 1515.
[29] M. Klimenkov, S. Nepijko, H. Kuhlenbeck, M. Bäumer, R. Schlögl and H.-J. Freund, Surf. Sci. 391 (1997) 27.
[30] R. Bouwman and P. Biloen, J. Catal. 48 (1977) 209.
[31] P. Lagarde, T. Murata, G. Vlaic, E. Freund, H. Dexpert and J.P. Bournonville, J. Catal. 84 (1983) 333.
[32] A. Fritsch and P. Légaré, Surf. Sci. 184 (1987) L355.
[33] H. Zuegg and R. Kramer, Appl. Catal. 9 (1984) 263.